REMOCEAN: A Flexible X-Band Radar System for Sea-State Monitoring and Surface Current Estimation

Francesco Serafino, C. Lugni, G. Ludeno, D. Arturi, M. Uttieri, B. Buonocore, E. Zambianchi, G. Budillon, and F. Soldovieri

***Abstract*—This letter deals with the use of the wave-radar REMOCEAN system for sea-state monitoring starting from images collected in the X-band at two different test sites. In particular, the measurement surveys were carried out at two coastal sites in the Gulf of Naples by means of the installation of the radar on a fixed and on a movable platform, respectively. The effectiveness of the system was also tested by means of a comparison between the REMOCEAN results and the high-frequency coastal radar observations, with emphasis to the sea surface current estimation.**

***Index Terms*—High-frequency coastal radar, image sequence analysis, marine X-band radar, sea-state monitoring, sea surface current estimation.**

I. Introduction

SEA STATE monitoring by X-band radar systems is becoming increasingly interesting, also due to its spatial resolution, which is much higher than the resolution of the relatively more common high-frequency (HF) coastal radars. In addition, compared to HF radar, X-band radar systems offer an improved operational flexibility; due to their small dimension, low weight, and easy installation, it is possible to install them even on a movable platform and from there to scan the sea surface with high temporal and spatial resolutions [1]–[6].

The operating principle of the X-band radar is based upon backscattering of electromagnetic signals by the sea surface roughness due to the effect of the Bragg resonance [3], [4]: This represent the "useful signal" to be processed when the aim is to achieve a spatial–temporal characterization of the sea state. In this framework, extensive data processing is necessary since modulation effects must be accounted for in the passage from the radar image to the desired spatial–temporal information about the sea state [3], [7]–[9]. In particular, data processing consists in solving a linear inverse problem where, starting from a series of spatial radar images collected at different time instants, the aim is to determine the elevation $\eta(x, y, t)$ of the sea surface as a function of the two horizontal spatial variables (related to the sea surface investigated by the radar) and of the time.

Here, we present the use of the wave-radar REMOCEAN system for the sea-state parameter estimation at two sites in the Gulf of Naples. In particular, the REMOCEAN system is concerned with the validation of a novel sea surface current estimation, which was numerically shown to achieve better performances compared to the least squares (LS)-based approach largely used in the literature [9], [10].

This letter is concerned with two main novel and interesting aspects associated to the presented measurement campaigns. The first one is represented by the use of the X-band radar system in a "mobile data acquisition modality," which allows to have a great flexibility in the choice of the observation point and is readily installed and operated; this could be of relevant interest in the case of crisis event monitoring and management. The second aspect is the comparison of the wave-radar system results with the information provided by an HF coastal radar operating in the Gulf of Naples [11], [12].

This letter is organized as follows. Section II presents the REMOCEAN system in terms of the technological solutions and the related data processing. Section III summarizes the setup and working principles of the HF coastal radar system. The two measurement campaigns are presented in detail in Section IV, where the results achieved by the REMOCEAN system are compared with the ones obtained by the HF-radar system. Finally, conclusions follow.

II. REMOCEAN System and the Data Processing

This section is devoted to briefly describe the REMOCEAN system by posing attention to both the hardware and the data processing. In particular, we report briefly the data processing approach, already detailed in [9] and [10], with the only aim to make the manuscript fully understandable and self-consistent.

The REMOCEAN system hardware consists of a CONSILIUM X-band radar radiating a maximum power of 12.5 KW and equipped with a 9-ft (2.74-m)-long antenna (see Fig. 1).

The data processing to extract from the X-band radar data the sea-state parameters (such as wave direction, wavelength, period, significant wave height, sea surface current intensity and direction, and temporal–spatial images of the sea surface elevation) is summarized as follows. As a first step, the raw data image sequence is transformed into a 3-D image spectrum by

Manuscript received September 26, 2011; revised November 27, 2011; accepted December 15, 2011. This work was supported in part by the MED TOSCA project, cofunded by the European Regional Development Fund and by the PROMETEO project, funded by the Campania Region. This work was also supported in part by the project HArBour traffIc opTimizAtion sysTem (HABITAT) under PON "Ricerca e Competitività 2007–2013."

F. Serafino, G. Ludeno, D. Arturi, and F. Soldovieri are with the Institute for Electromagnetic Sensing of the Environment, National Research Council, 80124 Napoli, Italy (e-mail: serafino.f@irea.cnr.it; ludeno.g@irea.cnr.it; daniele.arturi@libero.it; soldovieri.f@irea.cnr.it).

C. Lugni is with the INSEAN, the Italian Ship Model Basin, Department of Seakeeping and Maneuverability, National Research Council, 00128 Roma, Italy (e-mail: c.lugni@insean.it).

M. Uttieri, B. Buonocore, E. Zambianchi, and G. Budillon are with the Department of Environmental Sciences (DiSAm), "Parthenope" University, 80143 Napoli, Italy (e-mail: uttieri@uniparthenope.it; berardino.buonocore@uniparthenope.it; enrico.zambianchi@uniparthenope.it; giorgio.budillon@uniparthenope.it).

Color versions of one or more of the figures in this paper are available online at http://ieeexplore.ieee.org.

Digital Object Identifier 10.1109/LGRS.2011.2182031

Fig. 1. REMOCEAN system in mobile modality acquisition on the Gulf of Naples coast.

means of a 3-D Fast Fourier transform (3D-FFT), and the effect of the received signal power decay along the range, which has a smaller variability compared to the one associated to the phase of the signal, is filtered by applying a high-pass (HP) filter; the result is the image spectrum $F_I(k_x, k_y, \omega)$ [3], [5].

The second step aims at extracting the linear gravity wave components from the HP-filtered image spectrum $F_I(k_x, k_y, \omega)$. This filtering exploits the dispersion relation that links the wavenumber $\bar{k}$ to the angular frequency $\omega(\bar{k})$ through the sea surface current $U = (U_x, U_y)$ and the water depth h. The dispersion relation is given by

$$\omega(\vec{k}) = \sqrt{gk \tanh(kh)} + \vec{k} \cdot \tilde{U} \tag{1}$$

where g is the acceleration due to the gravity at the Earth's surface $k = |\vec{k}| = \sqrt{k_x^2 + k_y^2}$.

The current vector $\tilde{U} = (\tilde{U}_x, \tilde{U}_y)$ needs to be estimated before applying the dispersion relation in the filtering step [1], and several strategies have been implemented to pursue this aim [1]–[5], [9], [10]. The classical procedure is based on an LS approach presented in [1] and [5].

The REMOCEAN system exploits an innovative technique, which allows for a more accurate estimation of the surface current [9] as well as of the bathymetry [10]. This method determines the sea surface current as the quantity that globally maximizes the normalized scalar product (NSP) of the amplitude of the filtered image spectrum $|F_I(k_x, k_y, \omega)|$ and a characteristic function $G(k_x, k_y, \omega, U_x, U_y)$ accounting for the support of the dispersion relation in (1).

Once the current $\tilde{U} = (\tilde{U}_x, \tilde{U}_y)$ is estimated, it is possible to build the bandpass filter on the basis of the dispersion relation defined in (1) and apply it to the image spectrum $F_I(k_x, k_y, \omega)$; the result of the filtering procedure is the function $\tilde{F}_I(k_x, k_y, \omega)$. The third step is to move from the filtered radar image spectrum $\tilde{F}_I(k_x, k_y, \omega)$ to the desired sea-wave spectrum $F_W(k_x, k_y, \omega)$ by minimizing the effect due to the electromagnetic modulation phenomena [8]. This step is implemented by using the spectral modulation transfer function defined in [3]. Finally, the knowledge of the wave spectrum $F_W(k_x, k_y, \omega)$ permits to determine some parameters depicting the sea state; this is performed by generating the wavenumber directional spectrum, whose maximum provides the wavelength and propagation direction $[\lambda_p, \vartheta_p]$ of the dominant wave. The last step provides the evolution of the wave height $\eta(x, y, t)$ by performing an inverse 3D-FFT to the function $F_W(k_x, k_y, \omega)$.

III. HF Coastal Radar for the Study of Surface Currents and Sea State in the Gulf of Naples

The surface circulation and the wave field of the Gulf of Naples have been constantly monitored in real time since 2004 through a network of 25-MHz HF radars (SeaSonde systems manufactured by the CODAR Ocean Systems of Mountain View, USA) installed along the coasts of the basin and managed by the Department of Environmental Sciences (DiSAm) of the Parthenope University on behalf of AMRA scarl. The system provides a basin-scale synoptic reconstruction of the current field relative to the top 1 m of the water column, and at the same time, it enables to reconstruct the evolution of the wave field in an area adjacent to each antenna and extending offshore up to 12 km.

Similarly to X-band systems, HF radars also use gravity waves as target for electromagnetic signals emitted in the 3–30-MHz band, which corresponds to wavelengths from 10 to 100 m. In presence of a Bragg scattering, the backscattered echo recorded by the radar antenna, originated from waves traveling radially toward or away from it, yields a peak in the spectrum [13], with a Doppler shift with respect to the transmitted signal due to the action of a marine current beneath the wave field. The first-order Bragg peaks in the backscattered spectrum are used for the estimation of the radial component of current velocity; for this reason, the reconstruction of the vector current field in a given area requires at least two sites with overlapping coverage [14]. Through the second-order peaks, the wave parameters (significant height, period, and direction) can be extracted; this information can be retrieved by each antenna, which will therefore estimate a wave field relative to its neighborhoods. While almost no limit value is to be set for surface currents, the maximum recordable wave height h_{sat} is operationally limited by the operating frequency λ through the relationship $h_{\mathrm{sat}} = 2/k_0$ [m], where $k_0 = 2\pi/\lambda$ [m^{-1}] is the radar wavenumber [15]. For the 25-MHz system installed in the Gulf of Naples, $\lambda = 12$ m, and hence, $k_0 = 0.52$ m^{-1}, resulting in a limit wave height of $\sim$4 m. Such value is however compatible with the typical dynamics of the Gulf of Naples, and therefore, it does not represent a severe limitation to the usefulness of the system.

The first installation of the SeaSonde network in the Gulf of Naples comprised two remote stations, in Portici and Massa Lubrense (red triangles in Fig. 2), and a central unit at the Department of Environmental Sciences of the University of Naples "Parthenope." Since 2008, the network has been enhanced through the installation of a third antenna in Castellammare di Stabia. The resulting covered area extends for almost 900 km^2, up to 40 km from the coast. Each radar provides an hourly averaged radial map that is delivered in real time to the central unit, where the contributions from the three remote stations are then merged to create a total current map. Simultaneously, every single HF antenna processes wave data to 10-min-averaged wave fields over a sector centered on the antenna and extending up to 12 km offshore. To date, SeaSonde data in the Gulf of Naples have been used for oceanographic

TABLE I
MEASUREMENT PARAMETERS FOR THE FOUR DATA SETS

REMOCEAN System	Data set 1	Data set 2	Data set 3	Data set 4
Radar Rotation period (Δt)	1.48 sec	2.66 sec	2.66 sec	2.66 sec
Radar Image sampling (Δx)	7.9 m	3.5 m	7.9 m	13.8m
Minimum Range	700 m	700 m	700 m	1.5Km
Maximum range	1.5 nm	0.75 nm	1.5 nm	3 nm
Number of images	64	32	32	32
Actual angular sector	70°	70°	70°	115°
Antenna Height over sea level	20 m	20 m	20 m	60m

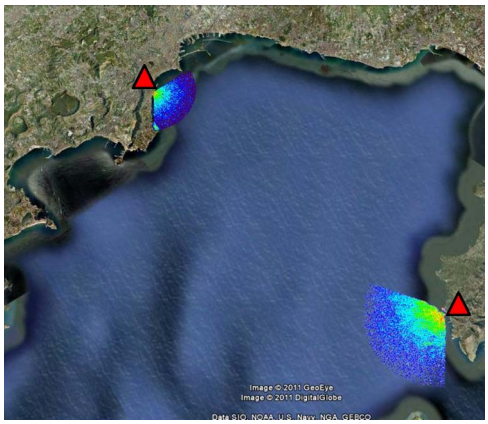

Fig. 2. Locations of the two X-band radar test sites in the Gulf of Naples. The red triangles indicate the position of two HF-radar antennas.

purposes, mostly focused at improving the knowledge of the circulation of the basin [11] and the effects of surface currents on the transport of passive tracers [12], [16]. The results so far recorded are in good agreement with previous reports (as discussed in [17]). This letter represents the first use of the HF-radar data to investigate the wave-field dynamics.

IV. MEASUREMENT CAMPAIGNS

This section is devoted to present the measurement campaigns carried out in the Gulf of Naples; Fig. 2 reports the location (image radar) of the test sites where the REMOCEAN system was installed and the positions of two of the three HF-radar systems.

In particular, the measurements were performed with three different observation ranges, 0.75 nm (1389 m), 1.5 nm (2778 m), and 3 nm (4167 m), and with a scanning angular sector of about 120° maximum. The details of the measurement parameters are given in Table I for this installation and for the below detailed data set 4.

The installation of the X-band radar was first carried out in Naples city (the upper left zone on Fig. 2). The localization of the radar platform (pos: LAT $= 40°49'29.00''$N, LON $= 14°13'15.89''$E) as well as the extent of the zone under investigation is detailed in Fig. 2. For this campaign, the radar was installed at a height of about 20 m above sea level, and the data were collected in two successive days of November (9th and 10th) 2010 (data sets 1 and 2) and one day of December (2nd) 2010 (data set 3).

It is worth noting that the measurement survey was very challenging since the investigated zone was a sea area closed at the southeast by the Ischia, Ponza, and Capri islands; this makes high wave height conditions less likely. Several oceanographic

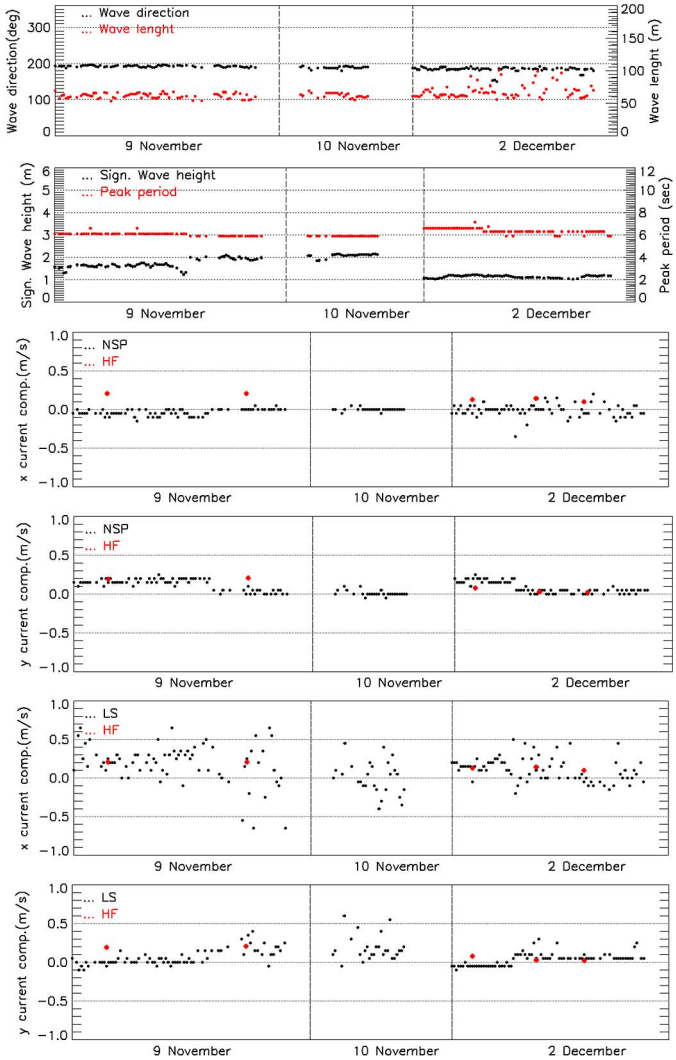

Fig. 3. Sea-state parameter estimates provided by the REMOCEAN system for the first site in Naples. The red diamonds represent the HF-radar measurements.

surveys carried out during the last decades in the Gulf of Naples (e.g., [18] and [19]) as well as the more recent HF-radar observations [11], [12] show that the most relevant forcing for the surface circulation, among the local factors, is the wind stress which generates currents up to 40 cm/s, about one order of magnitude greater than the mean basin circulation. For an updated review on the dynamics of the area, see [17].

Here, we present the results of the sea-state monitoring campaigns in terms of the main characteristic parameters as follows: wave direction θ_p (with respect to the Geographic North), peak period T_p, wavelength λ_p, significant wave height

TABLE II
STATISTICAL ANALYSIS OF THE SEA SURFACE CURRENT COMPONENT ESTIMATES

DATE	NSP				Least Squares				HF	
	μ_x(m/s)	μ_y(m/s)	stdev_x	stdev_y	μ_x(m/s)	μ_y(m/s)	stdev_x	stdev_y	μ_x(m/s)	μ_y(m/s)
9 Nov	-0.03	0.12	0.04	0.08	0.22	0.5	0.54	0.15	0.21	0.2
10 Nov	0.0	0.03	0.03	0.09	0.10	0.26	0.59	0.24	---------	----------
2 Dec	-0.01	0.08	0.08	0.07	0.06	0.22	0.35	0.19	0.12	0.04

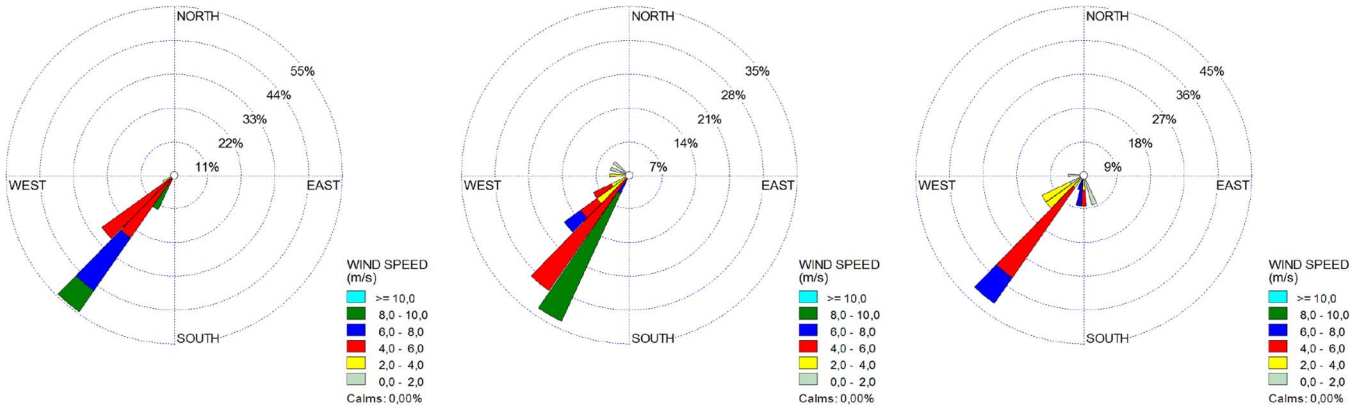

Fig. 4. Wind polar histograms reporting relative to (left panel) November 9, (middle panel) November 10, and (right panel) December 2, 2010.

$H_{1/3}$, and components of the sea surface current $U = (U_x\ U_y,)$ (with respect to the Geographic North).

Fig. 3 depicts the time series for data sets 1–3 in terms of the previously defined parameters; this figure shows only the "reliable measurements" not affected by rain. Fig. 3 also reports the sea surface current components $U = (U_x\ U_y,)$ estimated with the NSP (third and fourth panels) and LS (fifth and sixth panels) techniques, compared with the HF outcomes. This figure allows to point out that the estimations carried out with the NSP approach exhibit lower variance compared to the ones achieved by the LS approach; this behavior is more evident for the x-component of the sea surface current. The higher variance of the x-component of the sea surface current retrieved by REMOCEAN can be explained considering that the sea-wave motion is highly monodirectional, approximately along the y-axis; thus, there is a less sensitivity of the radar system in evaluating the x-component of the sea surface current. The good amount of available data has also permitted to perform a statistical analysis aimed at evaluating the variance of the more commonly applied LS compared with the here proposed NSP approach as far as the estimation of the two components of the sea surface current. The results are reported in Table II, where also the HF-radar results are presented; the better performances of NSP are pointed out by Fig. 3 and by the values of the standard deviation reported in Table II.

More importantly, Fig. 3 reports the good agreement of the sea surface current estimation by NSP with the HF-radar measurements described earlier in Section III. To make a reliable comparison, it is worth noting that the REMOCEAN system provides an estimate, obtained by analyzing the full area and, then, by assuming the currents to be spatially uniform in the acquired area, with a time interval of 1.5 min; differently, the HF-radar system provides an estimate given by the average of the measurements over a time interval of 75 min.

Fig. 4 depicts the polar histograms of the wind behavior (direction and speed) in the three days of measurements; the wind data were collected by the Acton DiSAm weather station

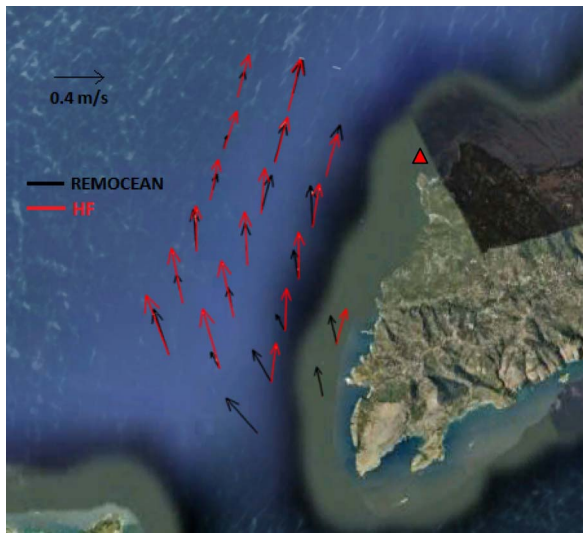

Fig. 5. Map of the sea surface currents estimated by REMOCEAN system and measured by the HF radar on February 17, 2010. The red triangle indicates the position of the HF-radar antenna.

located on the urban littoral of Naples (Lat.: 40° 50,19′ N, Long.: 014° 15,21′ E). They show a good correlation between the wind direction (220° with respect to the north) and the direction of the significant waves. The wind is strongest on November 9 and weakest on December 2; this behavior is consistent with the significant wave height seen in the second panel of Fig. 3.

Finally, we present a comparison between the results of the REMOCEAN system and of the HF radar in terms of spatial maps of the sea surface currents measured on February 17, 2011 (data set 4) at Massa Lubrense, with the southeast site highlighted in Fig. 2. Fig. 5 shows the sea surface currents as estimated from the two different radar systems, which are in very good agreement. In particular, Fig. 5 portrays a surface field characterized by a northward general current pattern. This

condition is often detected in this area and is associated with a northwestward-oriented Tyrrhenian coastal current.

V. Conclusion

This letter has presented the results of measurement surveys carried out with the REMOCEAN system in two test sites in the Gulf of Naples.

From the technological standpoint, the main interest lies in the adoption of a system installed on a movable platform; this feature is important since it offers a good flexibility in the choice of the spatial and temporal observation modalities.

From the scientific point of view, two main contributions can be pointed out. The first one stems out of the comparison of the REMOCEAN X-band radar system results with the ones provided by the HF-radar systems located in the Gulf of Naples. The comparison has allowed us to demonstrate the good performances of the X-band radar system in estimating sea state and surface currents.

The second aspect is represented by the analysis of the performances of the NSP strategy presented in [9], used on experimental data and compared with the classical LS approach available in the literature. For the sea surface current estimation, the adoption of the NSP approach has permitted to achieve more stable results, characterized by a smaller variance. As far as future developments, we plan to address the problem of the validation of the proposed approach for the bathymetry of coastal zones and the development of general strategies to mitigate the effect of the aliasing, which may arise when no proper time sampling is exploited in the measurements [20].

Acknowledgment

The authors would like to thank P. Falco and G. Zambardino of Department of Environmental Sciences (DiSAm) for their collaboration. The DiSAm of the "Parthenope" University operates the HF-radar system on behalf of AMRA scarl. The HF coastal radar remote sites are hosted by the ENEA Center of Portici, the Fincantieri shipyard in Castellammare, the "Villa Angelina Village of High Education and Professional Training." and the "La Villanella" resort in Massa Lubrense, whose hospitality is gratefully acknowledged.

References

[1] I. R. Young, W. Rosenthal, and F. Ziemer, "Three-dimensional analysis of marine radar images for the determination of ocean wave directionality and surface currents," *J. Geophys. Res.*, vol. 90, no. C1, pp. 1049–1059, 1985.

[2] F. Ziemer and W. Rosenthal, "Directional spectra from shipboard navigation radar during LEWEX," in *Directional Ocean Wave Spectra: Measuring, Modeling, Predicting, and Applying*, R. C. Beal, Ed. Baltimore, MD: Johns Hopkins Univ. Press, 1991, pp. 125–127.

[3] J. C. Nieto Borge, R. G. Rodriguez, K. Hessner, and I. P. Gonzales, "Inversion of marine radar images for surface wave analysis," *J. Atmos. Ocean. Technol.*, vol. 21, no. 8, pp. 1291–1300, Aug. 2004.

[4] J. C. Nieto Borge and C. Guedes Soares, "Analysis of directional wave fields using X-band navigation radar," *Coastal Eng.*, vol. 40, no. 4, pp. 375–391, Jul. 2000.

[5] J. C. Nieto Borge, "Analisis de campos de oleaje mediante radar de navegacion en banda X," Ph.D. dissertation, Univ. Madrid, Madrid, Spain, 1997.

[6] K. Hessner, K. Reichert, J. Dittmer, J. C. Nieto Borge, and H. Gunther, "Evaluation of WaMoS II wave data," in *Proc. 4th Int. Symp. Ocean Wave Meas. Anal.*, San Francisco, CA, 2000, pp. 221–230.

[7] P. H. Y. Lee, J. D. Barter, K. L. Beach, C. L. Hindman, B. M. Lade, H. Rungaldier, J. C. Shelton, A. B. Williams, R. Yee, and H. C. Yuen, "X-band microwave backscattering from ocean waves," *J. Geophys. Res.*, vol. 100, no. C2, pp. 2591–2611, 1995.

[8] W. J. Plant and W. C. Keller, "Evidence of Bragg scattering in microwave Doppler spectra of sea return," *J. Geophys. Res.*, vol. 95, no. C9, pp. 16 299–16 310, 1990.

[9] F. Serafino, C. Lugni, and F. Soldovieri, "A novel strategy for the surface current determination from marine X-band radar data," *IEEE Geosci. Remote Sens. Lett.*, vol. 7, no. 2, pp. 231–235, Apr. 2010.

[10] F. Serafino, C. Lugni, J. C. Nieto Borge, V. Zamparelli, and F. Soldovieri, "Bathymetry determination via X-band radar data: A new strategy and numerical results," *Sensors*, vol. 10, no. 7, pp. 6522–6534, Jul. 2010.

[11] M. Menna, A. Mercatini, M. Uttieri, B. Buonocore, and E. Zambianchi, "Wintertime transport processes in the Gulf of Naples investigated by HF radar measurements of surface currents," *Il Nuovo Cimento*, vol. 30 C, no. 6, pp. 605–622.

[12] M. Uttieri, D. Cianelli, B. Buongiorno Nardelli, B. Buonocore, P. Falco, S. Colella, and E. Zambianchi, "Multiplatform observation of the surface circulation in the Gulf of Naples (Southern Tyrrhenian Sea)," *Ocean Dyn.*, vol. 61, no. 6, pp. 779–796.

[13] D. E. Barrick, M. W. Evans, and B. L. Weber, "Ocean surface currents mapped by radar," *Science*, vol. 198, no. 4313, pp. 138–144, Oct. 1977.

[14] D. E. Barrick and B. L. Lipa, "An evaluation of least-squares and closed-form dual-angle methods for CODAR surface-current applications," *IEEE J. Ocean. Eng.*, vol. OE-11, no. 2, pp. 322–326, Apr. 1986.

[15] B. Lipa and B. Nyden, "Directional wave information from the SeaSonde," *IEEE J. Ocean. Eng.*, vol. 30, no. 1, pp. 221–231, Jan. 2005.

[16] B. Buonocore, D. Cianelli, P. Falco, R. Guida, M. Uttieri, G. Zambardino, and E. Zambianchi, "Hydrocarbon dispersal in the Gulf of Naples: Aparametric study," *Rapports Commission Int. pour l'Exploration Scientifique Mer Méditerranée*, vol. 39, p. 725, 2010.

[17] D. Cianelli, M. Uttieri, B. Buonocore, P. Falco, G. Zambardino, and E. Zambianchi, "Dynamics of a very special Mediterranean coastal area: The Gulf of Naples," in *Mediterranean Ecosystems: Dynamics, Management and Conservation*, G. S. Williams, Ed. New York: Nova Sci. Publ., 2012.

[18] M. Moretti, E. Sansone, G. Spezie, M. Vultaggio, and A. De Maio, "Alcuni aspetti del movimento delle acque del Golfo di Napoli," *Annali Istituto Universitario Navale*, vol. XLV–XLVI, pp. 207–217, 1976–1977.

[19] A. De Maio, M. Moretti, E. Sansone, G. Spezie, and M. Vultaggio, "Outline of marine currents in the Bay of Naples and some considerations on pollutant transport," *Il Nuovo Cimento*, vol. 8C, pp. 955–969, 1985.

[20] F. Serafino, C. Lugni, J. C. Nieto Borge, and F. Soldovieri, "Simple strategy to mitigate the aliasing effect in X-band marine radar data: Numerical results for a 2D case," *Sensors*, vol. 11, no. 1, pp. 1009–1027, 2011.